Supplemental Material: *Ab Initio* Electron-Phonon Interactions Using Atomic Orbital Wavefunctions

Luis A. Agapito and Marco Bernardi
Department of Applied Physics and Materials Science, Steele Laboratory, California Institute of Technology, Pasadena, California 91125, United States

1. BAND STRUCTURE INTERPOLATION IN SILICON USING ATOMIC ORBITALS AND WANNIER FUNCTIONS

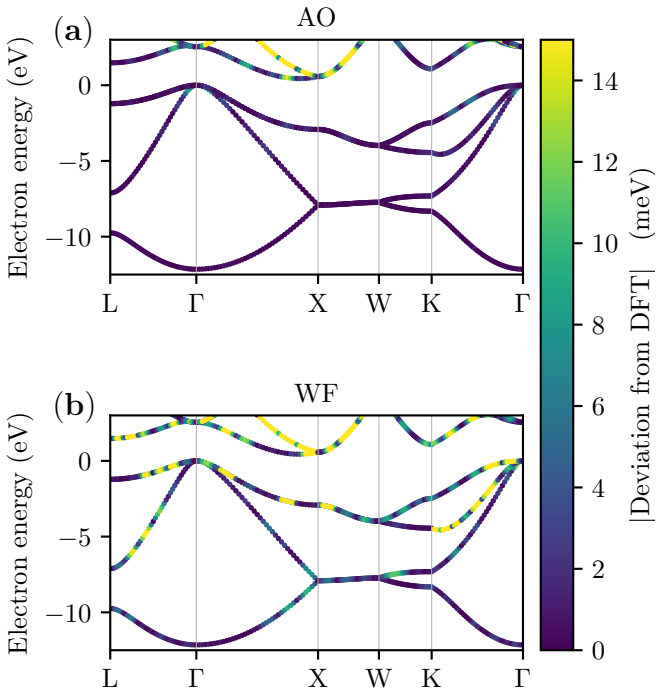

FIG. S1. Deviations from the DFT eigenvalues of the electronic eigenvalues obtained using AO (a) and WF (b) interpolations. Both interpolation methods employ Bloch electronic wavefunctions evaluated at a coarse $12\times12\times12$ **k**-point grid. The accuracy of the two methods is comparable.

2. BORON-DOPED DIAMOND

We use a diamond unit cell together with the virtual crystal approximation [1] to model the doping of diamond with boron. We employ a virtual atom $\langle \mathrm{BC} \rangle$ at every site with a composite pseudopotential that is the weighted average between those of boron and carbon. The norm-conserving pseudopotential of the virtual atoms is

$$\hat{V}^{\langle \mathrm{BC} \rangle} = x\hat{V}^{\mathrm{B}}_{\mathrm{loc}} + (1-x)\hat{V}^{\mathrm{C}}_{\mathrm{loc}} + \sum_{ij} \left|\beta^{\mathrm{B}}_i\right\rangle x D^{\mathrm{B}}_{ij} \left\langle\beta^{\mathrm{B}}_j\right| + \sum_{ij} \left|\beta^{\mathrm{C}}_i\right\rangle (1-x) D^{\mathrm{C}}_{ij} \left\langle\beta^{\mathrm{C}}_j\right|, \tag{S1}$$

where $\hat{V}_{\mathrm{loc}}$ is the local part of the pseudopotential, the nonlocal part is given in the Kleinman-Bylander form through the beta projectors $|\beta_i\rangle$ and coupling coefficients D_{ij}, and x is the boron fraction. We use a doping of one boron atom every 54 carbon atoms, which corresponds to $x = 0.0185185$. The DFT calculation shows a rigid shift of the band structure [Fig. S2(a)] with respect to the undoped case [Fig. S2(d)]; the system becomes slightly metallic, with the

Fermi level located 0.58 eV below the top of the valence band. The phonon dispersions show that the doping affects mostly the acoustic modes around Γ [Figs. S2(b) and (e)], in agreement with previous reports [2–4].

Fig. S2(c) shows the interpolated e-ph matrix elements for boron-doped diamond, computed using different coarse **q**-point grids and using the electronic states and phonon modes highlighted in Figs. S2(a) and (b). Different from undoped diamond, which is shown in Fig. 3(d) of the main text, we find a rapid convergence with increasing coarse **q**-point grid density of the interpolated e-ph matrix elements near Γ along the K−Γ direction [see the inset in Fig. S2(c)]. This behavior is due to the metallic character of boron-doped diamond, which eliminates the DFPT discontinuity at $\mathbf{q}=0$, as explained in the main text. Note that the discontinuity δ_2 near Γ is still present, since it is due to electron and phonon degeneracies, as discussed in the main text. If the same phonon modes as those in Fig. 8 of Ref. 4 are chosen (not shown), we obtain interpolated e-ph matrix elements in excellent agreement with Ref. 4.

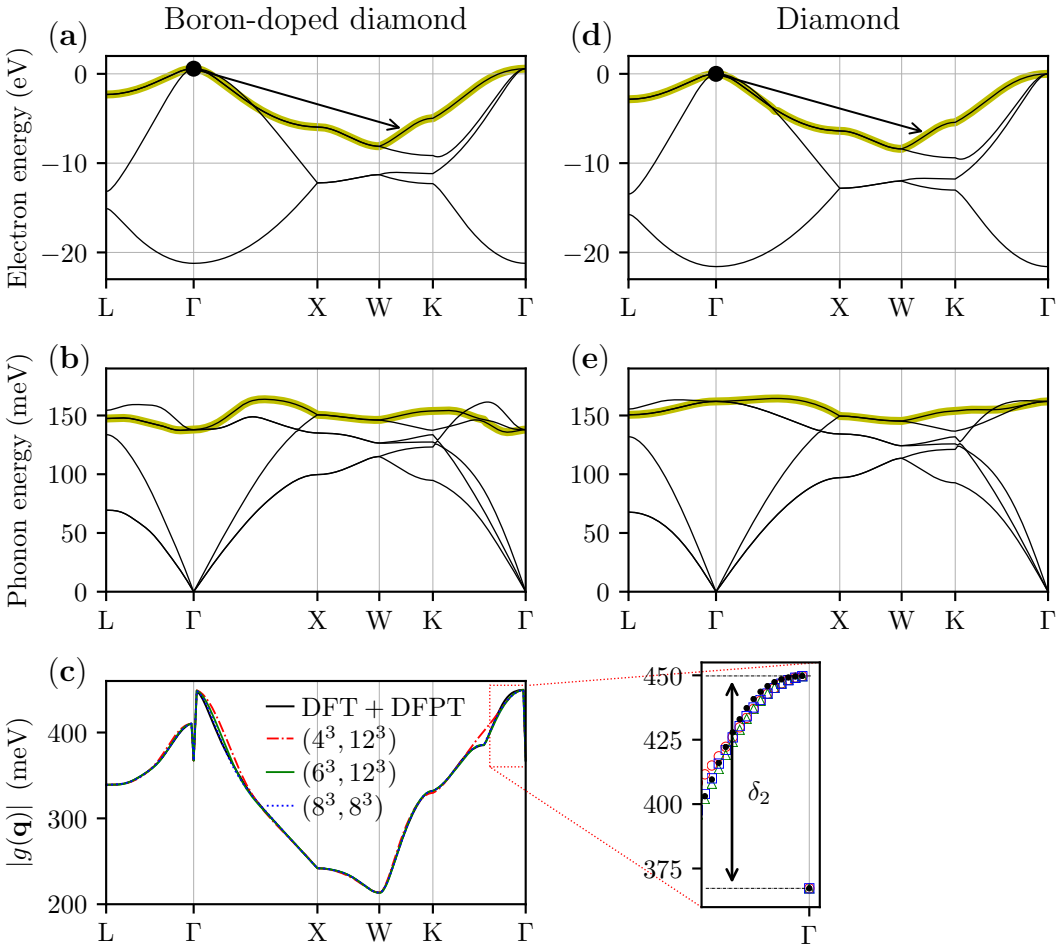

FIG. S2. Left panels: Interpolation of the e-ph matrix elements for boron-doped diamond using WFs. The selected electronic band and phonon mode are highlighted in (a) and (b), respectively. The DFT plus DFPT and interpolated e-ph matrix elements, for several ($\mathbf{q}_c$, $\mathbf{k}_c$) coarse grids, are given in (c). The inset zooms into the region near Γ. Right panels: the electronic band structure and phonon dispersions of pristine diamond are given for comparison.

TABLE S1. Difference (in meV units) between the DFT plus DFPT and the interpolated e-ph matrix elements in diamond at three high-symmetry points. The AO and WF interpolated results are given for several coarse grids.

$\mathbf{q}_f$ point	Method	Coarse grid size ($\mathbf{q}_c$ grid, $\mathbf{k}_c$ grid)		
		$(4^3, 12^3)$	$(6^3, 12^3)$	$(8^3, 8^3)$
K = $[-\frac{3}{8}, \frac{3}{8}, 0]$	AO	2.51	3.39	3.30
	WF	-0.59	0.17	0.00
L = $[0, \frac{1}{2}, 0]$	AO	-5.31	-5.31	-5.31
	WF	0.00	0.00	0.00
X = $[0, \frac{1}{2}, \frac{1}{2}]$	AO	-7.06	-7.06	-7.06
	WF	0.00	0.00	0.00

[1] N. Marzari, S. de Gironcoli, and S. Baroni, Phys. Rev. Lett. **72**, 4001 (1994).
[2] L. Boeri, J. Kortus, and O. K. Andersen, Phys. Rev. Lett. **93**, 237002 (2004).
[3] F. Giustino, J. R. Yates, I. Souza, M. L. Cohen, and S. G. Louie, Phys. Rev. Lett. **98**, 047005 (2007).
[4] F. Giustino, M. L. Cohen, and S. G. Louie, Phys. Rev. B **76**, 165108 (2007)